Hindawi
Geofluids
Volume 2022, Article ID 7236065, 14 pages
https://doi.org/10.1155/2022/7236065

Research Article

Study on Large Deformation Prediction and Control Technology of Carbonaceous Slate Tunnel in Lixiang Railway

Jinlong Yang

CCCC First Highway Engineering Group Co., Ltd., Beijing 100024, China

Correspondence should be addressed to Jinlong Yang; 33968711@qq.com

Received 29 April 2022; Revised 22 June 2022; Accepted 30 July 2022; Published 21 September 2022

Academic Editor: S. P. Pradhan

The construction of railway tunnel in carbonaceous slate environment is easy to cause rock mass disturbance, which leads to large deformation of surrounding rock and then threatens the safety of tunnel construction and operation. Therefore, based on the Wanlamu tunnel and Huajiaopo tunnel projects of Lixiang railway, combined with the regional geological conditions of the tunnel, and using the field monitoring technology and statistical principle, this paper analyzes the characteristics of tunnel surrounding rock pressure, secondary lining cracking, and initial support deformation under the conditions of different bedding slate. It is analyzed that the large deformation of carbonaceous slate surrounding rock is mainly related to the bedding, characteristics of surrounding rock, bias pressure, and the existence of high ground stress. The tunnel deformation is mainly manifested in peripheral convergence and vault settlement, and the peripheral convergence value is greater than the vault settlement value. In this study, the maximum daily convergence deformation of the tunnel peripheral convergence exceeds 117.8 mm, and the maximum convergence deformation can reach 951.7 mm, which is seriously affected by the slate bedding. According to statistics, more than 90% of the cross-section surrounding rock deformation of the tunnel with the slate bedding angle of 30° exceeds 600 mm. Then, based on BP neural network, the large deformation prediction model of railway tunnel under the carbon slate environment is constructed, and the accurate prediction of large deformation of carbon slate tunnel is realized, with the minimum prediction error of only 0.81%. It is pointed out that the main factors leading to the large deformation of the carbon slate tunnel are the lithology of the slate, the difficulty in predicting the deformation of the surrounding rock, and the failure of the initial support to close in time. The tunnel deformation can be effectively controlled by strengthening the geological work, optimizing the design parameters (enhancing the support stiffness, multiple support, and increasing the reserved deformation), and mining active reinforcement.

1. Introduction

With the rapid development of China's railway construction, more and more soft surrounding rocks are encountered in the construction process. Carbonaceous slate is one of them. As an extruded surrounding rock widely existing in the western region, it is widely distributed in the "Hexi Corridor Qilian Mountain West Qinling Mountain Longnan Wenchuan" high stress extrusion zone in China [1]. When the carbonaceous slate tunnel is integrated with the high ground stress environment, the phenomenon of large deformation of surrounding rock and damage and crack of support structure often occur after excavation. It has caused great trouble to the engineering construction. Therefore, correctly understanding the carbonaceous slate rock mass and accurately predicting the large deformation characteristics of slate are important prerequisites to solve the problem of large deformation in the process of slate construction [2, 3].

At present, there are many researches on the characteristics and mechanism of large deformation of soft rock, and many achievements have been made. By analyzing the deformation mechanism of a large number of typical high stress soft rock tunnels, Yan and Yi, Weidong et al., and Li et al. [4–6] summarized three main deformation mechanisms: plastic flow pattern of soft rock, wedge extrusion of structural type, and bending of plate beam. Aiming at the research on the large deformation mechanism of slate, Yunlong and Zhongsheng [7] put forward the large deformation

and collapse evolution model of carbonaceous slate under the bending mechanism of plate beam based on the large deformation of surrounding rock in the carbonaceous slate section of Muzhailing railway tunnel. By analyzing the deformation mechanism of the slate section of Maoyushan tunnel, Jun [8] pointed out that the interlacing of argillaceous slate and calcareous slate and great differences in mechanical properties are the main factors of large deformation, and the deformation mechanism is mainly manifested in shear sliding along the structural plane. Zhang et al., Takeda et al., Chen et al., and Iwano [9–12] collected the tunnel deformation characteristics under different excavation methods and studied the influence of excavation methods on the large deformation of soft rock tunnel. Weidong et al., Guo et al., Wu et al., and Ren et al. [5, 13–15] studied different tunnels with the same excavation method and pointed out that the deformation characteristics of high stress soft rock tunnel are diverse, with remarkable characteristics such as fast deformation rate, long deformation time, and large total deformation. On this basis, Yuan, Fang et al., and Pan and Cheng [16–18] gave reasonable construction control measures based on the characteristics and genetic mechanism of large deformation and failure of tunnels in different soft slate strata in different regions, so as to provide reference for the construction of similar slate tunnels. Li et al. [19, 20] studied the mechanical behavior of the tunnel during large deformation by means of on-site monitoring and numerical analysis and carried out the research on prevention countermeasures. Rao et al., Ma et al., and Bian et al. [21–23], based on the field monitoring data of large deformation of soft rock tunnel, with the help of different prediction models, carried out the prediction research of large deformation of tunnel, effectively grasped the development trend of tunnel deformation, and verified the feasibility of different models in the prediction of large deformation of tunnel, but the prediction accuracy is limited and the practicability is limited. Therefore, it is necessary to further study it.

In the above research, the research contents are generally separated from each other, and the relationship between deformation amount, deformation characteristics, and deformation mechanism is not effectively established, which is lack of integrity. At the same time, in view of the different existing environments of specific tunnel projects, there are differences in the main characteristics of deformation and the main control mechanism, and the prediction method is relatively simple and cannot be popularized. Therefore, based on the idea of combination prediction model, this paper constructs an integrated combination prediction model of chaos optimization, summarizes the characteristics of large deformation of tunnel, analyzes the causes of large deformation of surrounding rock and the characteristics of initial support deformation, constructs a combination prediction model of large deformation of tunnel on the basis of test section, and puts forward relevant technical measures for large deformation tunnel construction, in order to solve the problems of unpredictable deformation size and uncontrollable deformation mode of tunnel construction in carbonaceous slate environment.

2. Project Overview

The Wanlamu tunnel and Huajiaopo tunnel of Lijiang-Shangri-La railway are located in the western boundary fault zone (Jinshajiang-Zhongdian fault zone) of the Sichuan-Yunnan rhombic fault block on the southeast edge of the Qinghai-Tibet Plateau formed by the collision and convergence of the Eurasian plate and the Indian Ocean plate. They belong to the western Yunnan seismic belt in the southern section of China's famous north-south seismic belt. The geological structure is complex, the neotectonic movement is strong, and the stress concentration is high. There is high ground stress in the geological environment of multistage magma intrusion, rock burst may occur in hard and brittle lithology, and large deformation may occur in soft rock. The ground elevation of the line travel area is 2550 m~3630 m, and the design elevation of the line is greater than 2500 m. The geological conditions of tunnel surrounding rock are complex, the construction safety risk is very high, and the construction is difficult. The mountains and valleys along the line are high and deep; the terrain is complex; deep and large active faults are developed; neotectonic movement and seismic activity are strong; the rock mass is broken and loose; the adverse geology such as landslide, collapse, and staggered fall are dense, wide, and distributed in groups; and the adverse geological problems such as debris flow, karst, gas, and high ground stress are very prominent.

3. Analysis of Deformation Characteristics of Carbonaceous Slate

The magnitude, rate, and depth of surrounding rock deformation are the basic data used to evaluate the stability of tunnel surrounding rock. They are also the basic parameters for the dynamic design of tunnel surrounding rock support and the evaluation of support effect. The monitoring and measurement data of Wanlamu tunnel and Huajiaopo tunnel of Lixiang railway are shown in Table 1. The tunnel face accident are shown in Figure 1. According to the statistical analysis of geological exploration data, observation inside and outside the tunnel, and field monitoring measurement data, it is found that the deformation characteristics of carbonaceous slate tunnel in this paper have the following characteristics.

3.1. Large Tunnel Deformation. The monitoring results of high-precision total station and peripheral convergence meter are shown in Figure 2, and the on-site deformation of tunnel is shown in Figure 3. It can be seen from Figures 2 and 3 that under the influence of the vertical pressure of surrounding rock and the self-weight of initial support, the maximum displacement of arch crown is as high as 869.5 mm and the maximum convergence deformation is as high as 951.7 mm. Due to the improper selection of support time and the reserved deformation of support, the I-beam is excessively distorted. At the same time, there are serious safety and quality hidden dangers in the shear failure and fracture of arch crown, which is easy to cause tunnel face collapse and arch crown collapse. It poses a great threat to the life and property safety of engineering and construction personnel.

Table 1: Tunnel site monitoring and measurement data.

Monitoring section	Peripheral convergence value (mm)	Convergence time (d)	Vault settlement value (mm)	Settlement time (d)	Bedding dip (°)
D1K87+060	870.6	47	663.4	48	15.0
D1K87+070	661.7	49	512.3	42	30.0
D1K87+090	923.5	53	649.4	50	30.0
D1K87+100	546.9	48	551.7	46	45.0
D1K87+110	712.5	51	687.5	48	0.0
D1K87+120	694.3	48	684.2	50	30.0
⋮	⋮	⋮	⋮	⋮	⋮
D1K87+480	341.5	42	320.1	41	0.0
D1K87+490	406.7	44	387.4	39	45.0
D1K87+500	319.8	46	331.5	43	30.0
D1K87+510	734.2	51	621.8	55	30.0
D1K87+520	921.9	55	754.4	52	35.0
D1K87+530	655.8	49	532.2	38	45.0

Note: due to space reasons, only some section monitoring and measurement data are listed randomly.

Figure 1: Tunnel face accident.

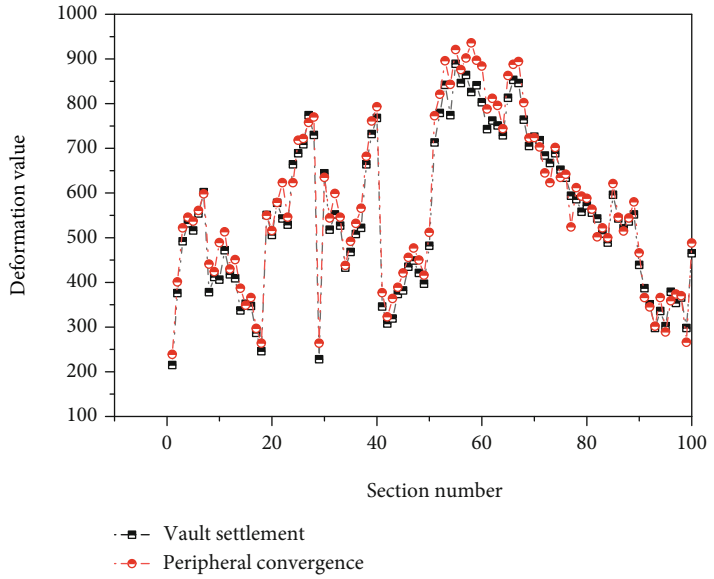

Figure 2: Tunnel deformation data.

3.2. Long Tunnel Deformation Time. Under the geological origin of primary structural plane and secondary structural plane, the stress state of carbonaceous slate has changed greatly under the influence of excavation. From Table 1 and Figures 4 and 5, it can be seen that the deformation of the tunnel is characterized by long time and large

Figure 3: Tunnel deformation.

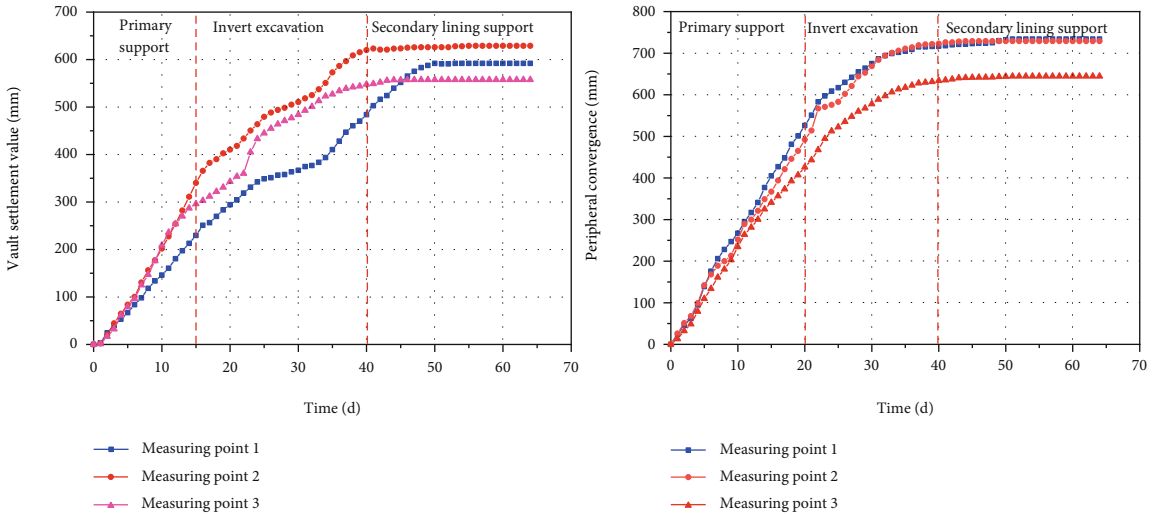

Figure 4: Crown settlement/peripheral convergence duration curve.

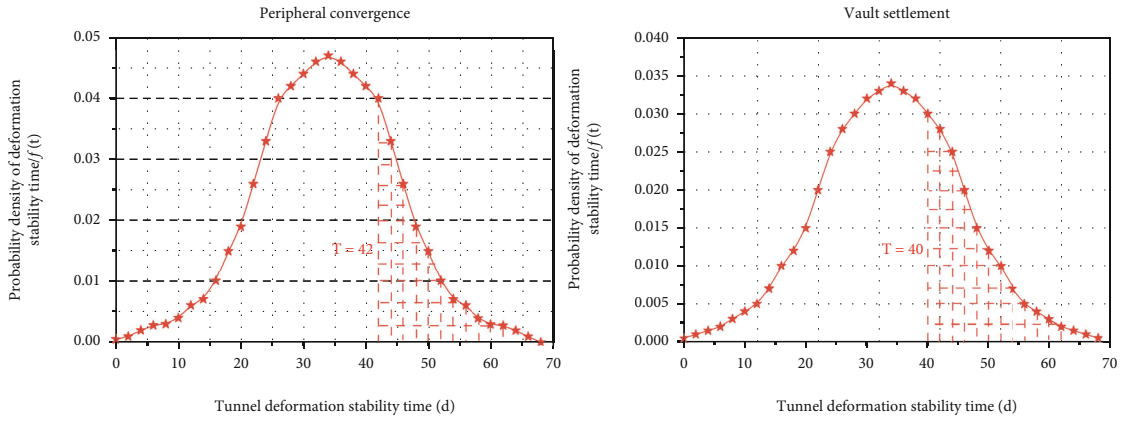

Figure 5: Normal distribution curve of vault settlement/peripheral convergence stability time.

deformation span. The duration curve is divided into three stages: first, the surrounding rock rapidly produces elastic deformation under unloading, which is also known as the elastic stage of large deformation of soft rock. In this paper, the maximum daily deformation of the tunnel is 117.8 mm, and the average daily deformation is 30.0 mm. However, the duration of this stage is different. The shortest time of some sections is only 5 days, and the longest time can be up to 2 weeks. After the first stage of deformation release, when the surrounding rock stress is less than the initial support, the surrounding rock deformation gradually changes from elastic to plastic deformation, the daily deformation rate of surrounding rock decreases, and the maximum daily deformation per day is controlled at 20.0 mm, but the duration is long, and the average duration is more than 4 weeks. The last stage is the surrounding rock stability stage. Under the action of various support conditions, the surrounding rock of the tunnel basically converges and stabilizes, the deformation rate approaches 0, and the final stability time is about 70 days.

3.3. Significant Stress Concentration at Arch Foot. Under the action of the special shape of the tunnel, affected by the deformation of surrounding rock and the horizontal and vertical load of surrounding rock, the stress concentration at the arch foot of the tunnel is significant, which is manifested in the distortion of I-beam and connecting plate, the excessive internal force of arch frame, the crushing of surrounding rock at the arch foot by extrusion pressure, and even tunnel collapse and other accidents in serious cases.

3.4. Deformation Is Significantly Affected by High Collapse Ratio. Lixiang railway is a single track railway. The height span ratio of tunnel structure is relatively large (about 1.4), and the rise span ratio of side wall is small (about 1/15), which is not conducive to horizontal convergence control. During the initial stage of excavation, the deformation of the tunnel is mostly measured in the lower arch, and the deformation of the lower arch is small according to the monitoring data of the initial stage of excavation (the deformation of the lower arch is mostly measured in the lower arch, and the deformation of the lower arch is small according to the monitoring data of the lower arch).

3.5. Deformation Is Significantly Affected by Bedding. At present, with the deepening of tunnel research and the application of NATM, the surrounding rock of the tunnel has been regarded as the main bearing structure. During the design and construction, the self-supporting capacity of the surrounding rock can be brought into full play and combined with the support system, which can form a better balance between the surrounding rock and the support system and ensure the safety of the tunnel during construction and service. Surrounding rock acts as load, material, and bearing, which is also different from ground structures. From this structural feature, the study of tunnel stability must start with the study of surrounding rock. Therefore, it is necessary to study the stability of the surrounding rock of the main bearing body in the tunnel engineering, especially for the bedding rock mass; it is very necessary to analyze its impact on the surrounding rock of the tunnel. Taking the slate exposed in the single track railway tunnel of Lixiang railway as an example, the cleavage failure morphology of carbonaceous slate is significantly affected by bedding, which can be divided into tensile failure, shear failure, and tensile shear combined failure between matrix and bedding planes. Moreover, the failure modes of bedding at different angles are also quite different. Through analysis, the displacement value of the tunnel is the largest under the condition of 30.0° bedding angle. According to statistics, more than 90% of the cross-section surrounding rock deformation of the tunnel with a slate bedding angle of 30° is more than 600 mm, which once again reflects the impact of the tunnel slate bedding on the tunnel surrounding rock deformation.

4. Deformation Prediction and Analysis of Carbonaceous Slate

4.1. Rolling Prediction Model of Carbonaceous Slate Deformation. According to the characteristics of large deformation of carbonaceous slate tunnel, this paper combines genetic algorithm (GA) and BP neural network to establish a GA-BP neural network model, which is used to predict the surrounding convergence field monitoring data with large deformation and obvious deformation law. BP neural network usually refers to a multilayer feedforward neural network based on error backpropagation algorithm (BP algorithm). In the learning process, the algorithm can reduce the error function in the fastest direction, and its iterative calculation formula can be expressed as

$$h_{k+1} = h_k - s_k g_k, \tag{1}$$

where h_k is the current weight and deviation, h_{k+1} is the weight and deviation of the next neuron generated, s_k is the learning rate, and g_k is the gradient.

In this paper, it is assumed that the network training sample set is $\{X_i, Y_j\}$, it is the input of the neural network is $[x_1, x_2, \cdots, x_i, \cdots, x_I]^T$, and x_i represents the monitoring value of peripheral convergence on the ith day of the tunnel. The output of the neural network is $[y_1, y_2, \cdots, y_j, \cdots, y_J]^T$, and y_j represents the predicted value of peripheral convergence on the j day of the tunnel. Then, there are:

(1) Forward transmission of BP neural network signal

The calculation formula for calculating the output signal of the neuron in the hidden layer in BP neural network is

$$v_l = f_1\left(\sum_{i=1}^{I} w_{il} x_i - a_l\right), \quad l = 1, 2, \cdots, L. \tag{2}$$

In BP neural network, the calculation formula for calculating the output signal of the first neuron in the output layer is

$$y_j = f_2\left(\sum_{j=1}^{J} w_{jk} v_i - b_j\right), \quad j = 1, 2, \cdots, J. \tag{3}$$

The error function of the corresponding sample under the incremental processing mode is defined as follows:

$$E = \frac{1}{2}\sum_{j=1}^{J}\left(y_j - O_{ij}\right)^2. \tag{4}$$

(2) Error backpropagation and weight threshold update

The calculation formula of the incremental connection between the weights of the neurons in the lth neural network is updated from the incremental connection between the weights of the neurons in the jth neural network:

$$\Delta w_{lj} = -\eta\frac{\partial E}{\partial w_{lj}} = -\eta\frac{\partial E}{\partial y_j}\cdot\frac{\partial y_j}{\partial w_{lj}} = \eta\left(O_{ij} - y_j\right)\cdot f_2{}'\cdot v_l. \tag{5}$$

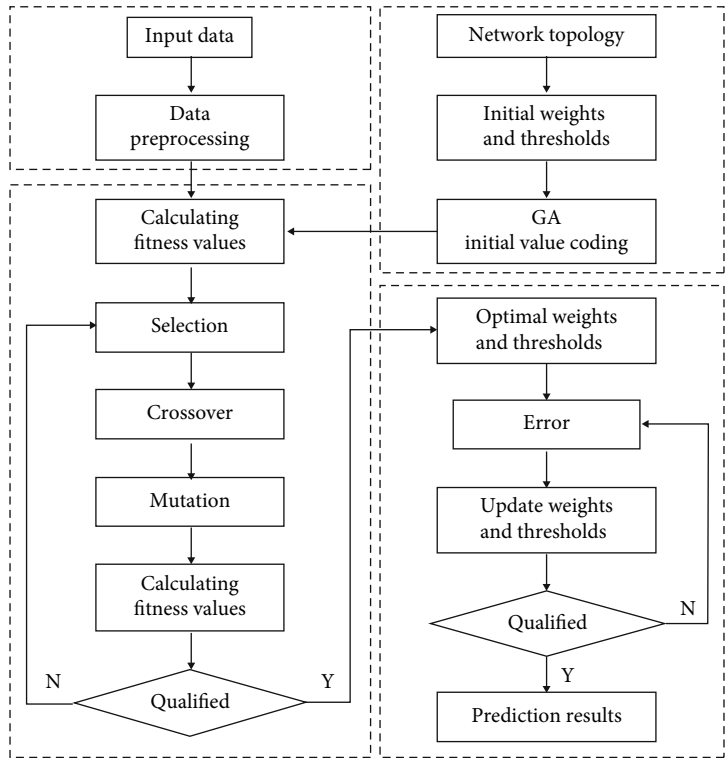

Figure 6: GA-BP neural network algorithm flow.

For the connection weight between the mth neuron in the input layer and the th neuron in the hidden layer of BP neural network, the incremental calculation formula of the connection weight between the two neurons is as follows:

$$\begin{aligned}\Delta w_{il} &= -\eta \frac{\partial E}{\partial w_{il}} = -\eta \sum_{j=1}^{J} \frac{\partial E}{\partial y_j} \cdot \frac{\partial y_j}{\partial v_l} \cdot \frac{\partial v_l}{\partial w_{ml}} \\ &= \eta \sum_{j=1}^{J} \left(O_{ij} - y_j\right) \cdot f_2{}' \cdot w_{lj} \cdot f_1{}' \cdot x_i.\end{aligned} \tag{6}$$

(3) Network weight threshold update

According to the content described above, calculate the change increment of the weight and threshold of each layer of neurons in BP neural network after each iteration, and use the obtained increment to correct the weight and threshold of each layer of neurons for the next network learning process; that is, the update formula of each training sample $i \in \{1, 2, \cdots, N\}$ is

$$\begin{cases} b_j \longleftarrow b_j + \Delta b_j, \\ w_{lj} \longleftarrow w_{lj} + \Delta w_{lj}, \\ \forall j = 1, 2, \cdots, J, l = 1, 2, \cdots, L, \end{cases} \tag{7}$$

$$\begin{cases} a_j \longleftarrow a_j + \Delta a_j, \\ w_{li} \longleftarrow w_{li} + \Delta w_{li}, \\ \forall i = 1, 2, \cdots, I, l = 1, 2, \cdots, L. \end{cases} \tag{8}$$

Genetic algorithm is an optimization search algorithm based on the principles of natural selection and genetic genetics. Using GA to optimize the weight and threshold of BP artificial neural network can improve the performance of BP neural network, overcome the local minimum, and then improve the network learning accuracy. The algorithm flow chart of the GA-BP neural network is shown in Figure 6.

4.2. Analysis of Prediction Results of Convergence Deformation of Carbonaceous Slate. It can be seen from Table 1 and Figure 5 that the convergence and stability time around the tunnel is concentrated in about 45 days after tunnel excavation; that is, after 45 days of tunnel excavation, the surrounding rock is basically stable; that is, the convergence value around the tunnel reaches the maximum. In order to fully verify the rolling prediction ability of the prediction model, the prediction process is divided into three types: early stage, medium-term, and late stage prediction: in the early stage, the monitoring and measurement data in the first stage of 1~15 days are used as training samples, and 16~20 days are used as verification samples. In the middle stage, 1~30 days were used as training samples, and 31~35 days were used as verification samples. In the later stage, 1~40 days were used as training samples, and 41~45 days were used as verification samples. The prediction results

Table 2: Forecast results of the previous period.

Monitoring cycle (d)	Peripheral convergence (mm)	BP neural network model		GA-BP neural network model	
		Estimate (mm)	Relative error (%)	Estimate (mm)	Relative error (%)
16	427.4	441.2	3.23	438.0	2.48
17	448.6	465.4	3.74	457.9	2.07
18	481.3	497.2	3.30	492.0	2.22
19	501.2	516.0	2.95	513.6	2.47
20	526.5	540.6	2.68	538.2	2.22
Average relative error			3.18		2.29

Table 3: Medium term forecast results.

Monitoring cycle (d)	Peripheral convergence (mm)	BP neural network model		GA-BP neural network model	
		Estimate (mm)	Relative error (%)	Estimate (mm)	Relative error (%)
31	686.2	669.4	2.45	696.7	1.53
32	694.7	707.9	1.90	702.6	1.14
33	699.2	713.8	2.09	710.6	1.63
34	702.5	719.4	2.41	711.8	1.32
35	705.6	721.8	2.30	713.9	1.18
Average relative error			2.23		1.36

Table 4: Later prediction results.

Monitoring cycle (d)	Peripheral convergence (mm)	BP neural network model		GA-BP neural network model	
		Estimate (mm)	Relative error (%)	Estimate (mm)	Relative error (%)
41	718.2	732.4	1.97	724.1	0.81
42	720.6	735.9	2.12	727.3	0.93
43	721.4	737.8	2.27	728.9	1.03
44	722.5	738.9	2.27	730.4	1.09
45	723.7	740.1	2.27	730.8	0.98
Average relative error			2.18		0.97

are compared with BP neural network. Taking d1k87+510 section as an example, the model prediction results of each stage are shown in Tables 2–4 and Figures 7 and 8.

It can be seen from Tables 2–4 and Figures 7 and 8 that in the prediction of convergence monitoring data around carbonaceous slate tunnel, whether in the early result prediction, medium-term, and late result prediction, the prediction accuracy of GA-BP neural network prediction model is higher than that of BP neural network prediction model, and the prediction accuracy in the later stage is higher than that in the middle and early stage, indicating that the prediction accuracy of the prediction model is higher with the increase of the amount of data. The minimum prediction error in the early stage is only 2.07%, and the average error is 2.29%, which is 27.99% lower than the average relative error of BP neural network prediction model. The later prediction results and error is shown as Figure 9. The minimum prediction error in the later stage is 0.81%, and the average error is 0.97%, which is 55.50% lower than the average relative error of BP neural network prediction model. It not only verifies that the prediction accuracy of GA-BP neural network prediction model is higher than that of traditional BP neural network prediction model, especially when there is enough data, GA-BP neural network prediction model can greatly improve the prediction accuracy of the model, but also verifies the applicability of GA-BP neural network prediction model in the prediction of convergence deformation around carbonaceous slate tunnel.

Figure 10 reflects the variation law of error loss of different neural network prediction models in the process of tunnel deformation prediction. It can be seen from the figure that the variation law of error loss of GA-BP neural network prediction model is basically the same, showing a trend that the initial error is large, but the error loss gradually decreases with the increase of the number of network training iterations. However, in the change of error loss of BP neural network prediction model, the change law of error loss is not obvious, and the initial value of error is also large. However, with the increase of network training iterations, there is a phenomenon of polarization. One is that the error loss gradually decreases and tends to be stable, and the other gradually increases with the increase of iterations. Although it

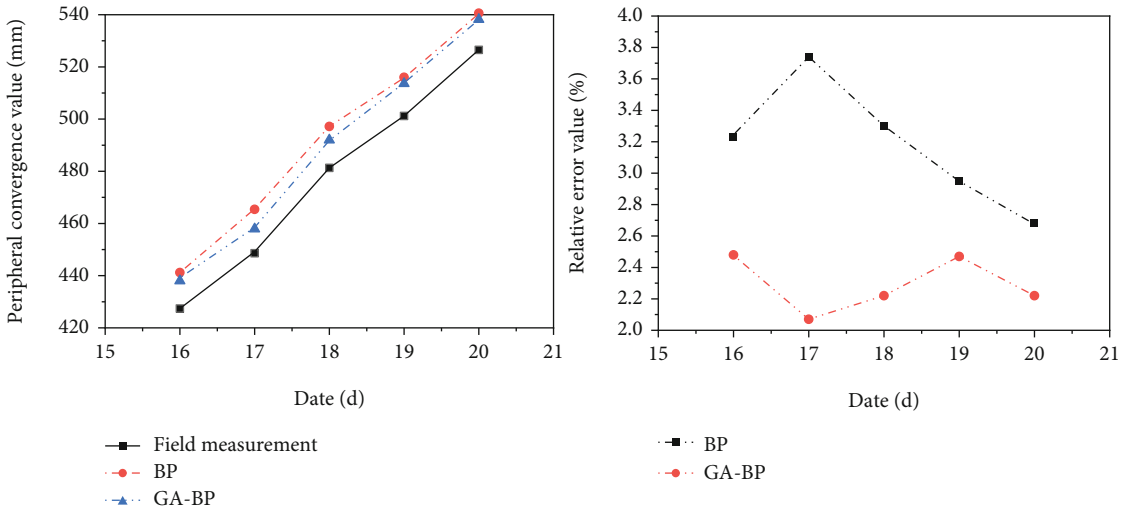

Figure 7: Early prediction results and errors.

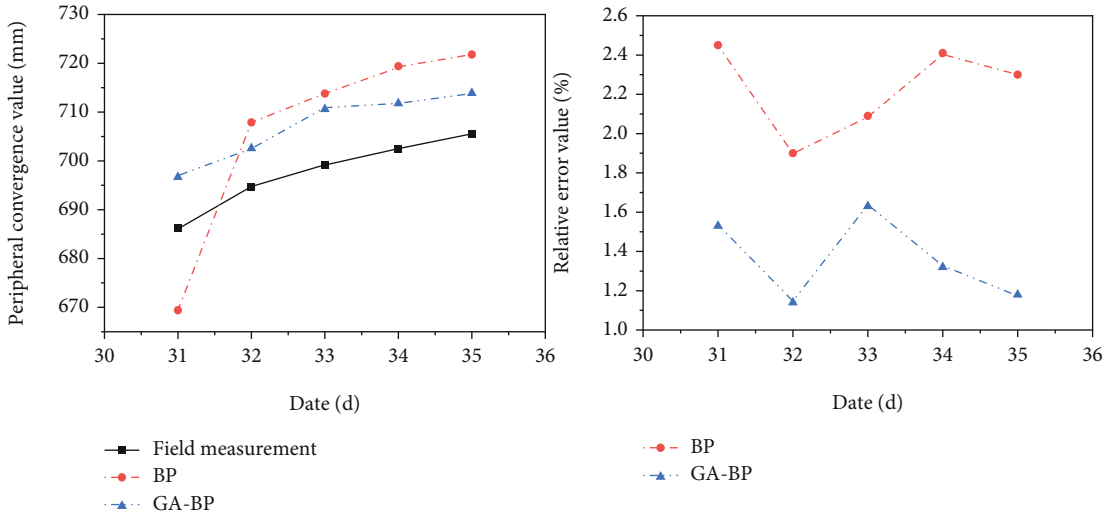

Figure 8: Medium term forecast results and errors.

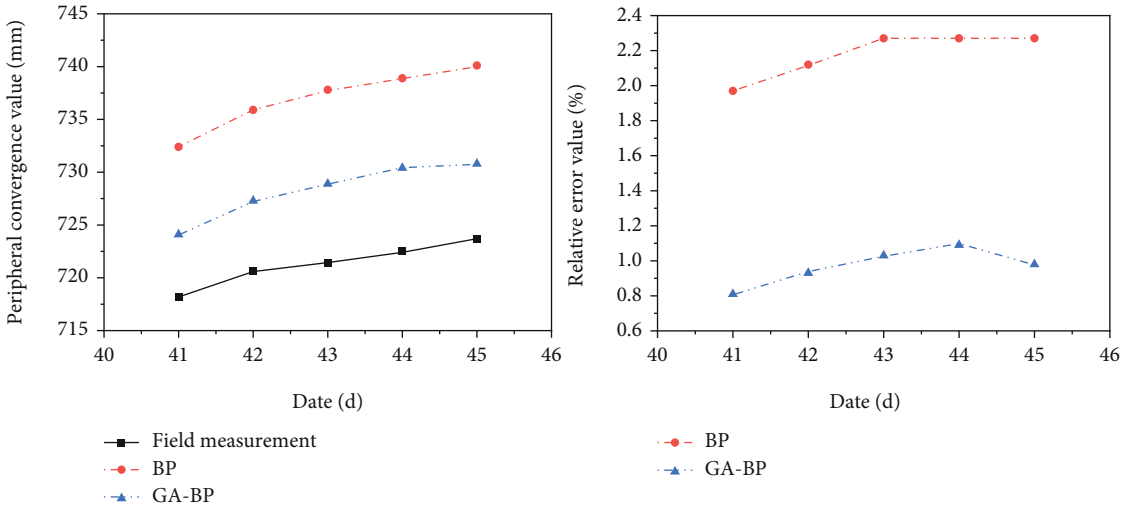

Figure 9: Later prediction results and errors.

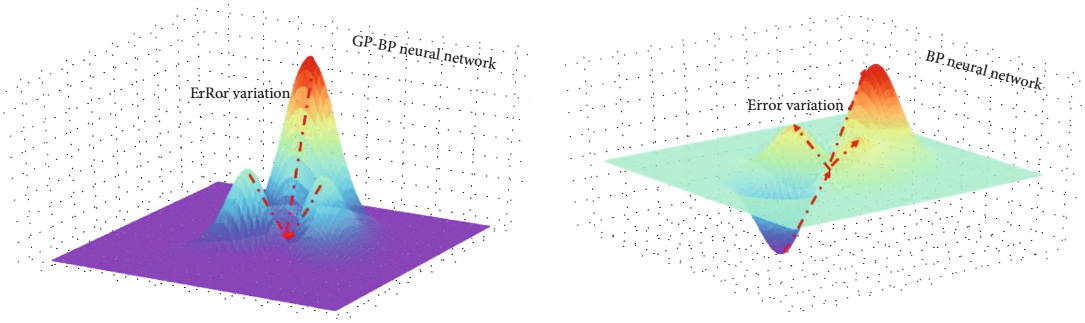

Figure 10: Variation law of error loss of different models.

eventually tends to be stable, the overall error loss is large, which is difficult to reflect the real error value of model prediction. As a result, the prediction error of the model is large and the accuracy is reduced. The superiority of GA-BP neural network prediction model in the prediction of convergence deformation around carbonaceous slate tunnel is verified again.

5. Control Measures for Large Deformation Tunnel in Carbonaceous Slate

5.1. Strengthen Geological Exploration, Make Statistics of Tunnel Deformation Law, and Predict Large Deformation Area. In view of the large deformation of the carbonaceous slate tunnel of Lixiang railway, it is suggested to strengthen the geological exploration of the tunnel project under construction under the relevant geological environment. At the same time, during tunnel excavation, the monitoring measurement and law statistics of the tunnel should be increased, and the large deformation of the tunnel should be predicted according to the monitoring measurement data, so as to select a reasonable support time and take reasonable support means to prevent the occurrence of construction accidents caused by the untimely prediction of large deformation.

Firstly, the mathematical statistics method is used to process the tunnel deformation data, and then, the reserved deformation of the tunnel is preliminarily determined.

When the square difference σ^2 of the distribution function is unknown, since the sample variance S^2 is an unbiased estimate of the overall distribution variance σ^2, there are

$$\sigma^2 S^2 \frac{\bar{X} - \mu}{S/\sqrt{n}} \sim t(n-1), \tag{9}$$

where $\bar{X}$ is the mean value of statistical samples, μ is the average value of overall distribution, n is the number of samples, and $t(n-1)$ is the distribution function.

Then, the confidence level of the average value of tunnel deformation is $(1-\alpha)$, and a confidence interval is

$$\left(\bar{X} - \frac{S}{\sqrt{n}} t_{\alpha/2}(n-1), \bar{X} + \frac{S}{\sqrt{n}} t_{1-\alpha/2}(n-1)\right). \tag{10}$$

The interval estimation of tunnel deformation is shown in Figure 11. It can be seen from Figure 11 that $z_{\alpha/2}$ and $z_{1-\alpha/2}$ are the quantiles of normal distribution. For random sampling of tunnel deformation under a large deformation level, the probability that the average value X is located in $(z_{\alpha/2}, z_{1-\alpha/2})$ under the condition of ensuring accuracy and reliability, take $1-\alpha = 95\%$, and take the upper and lower limits of the confidence interval to preliminarily determine the reserved deformation of the tunnel.

In order to verify the prediction accuracy of the prediction model constructed in this paper in the large deformation area, 30 groups of slate bedding with peripheral convergence of more than 600.0 mm in Wanlamu tunnel and Huajiaopo tunnel of Lixiang railway were simulated and predicted at 30.0°. The simulation results of convergence deformation in three phases (early, middle, and late) are shown in Figure 12.

5.2. Increase the Support Stiffness and Reasonably Increase the Reserved Deformation according to the Prediction Results. Based on the lithology and hydrogeological characteristics of the project and the actual situation of the environment, it is difficult to control the deformation by using conventional support parameters. Therefore, in the later construction, multiple supports shall be adopted, with emphasis on the elliptical section with good stress, increasing the curvature of the initial support of the side wall, increasing the reserved deformation, and lengthening the system anchor bolt. According to the later construction statistics, when the original support method is adopted for the class V surrounding rock of the tunnel body, the deformation is generally more than 600 mm, and the deformation of class V reinforced surrounding rock is also more than 600 mm. The resulting accidents such as steel arch foot bending deformation (Figure 13) and initial support damage (Figure 5) occur from time to time, which are all large deformation surrounding rock. Therefore, it is considered to optimize its support parameters. The optimized tunnel support parameters are shown in Table 5.

Practice has proved that measures such as multiple support, increasing support stiffness, and increasing reserved deformation are effective in controlling large deformation. The number of deformation and damage of tunnel initial support, steel arch, and other support measures is significantly reduced compared with that before.

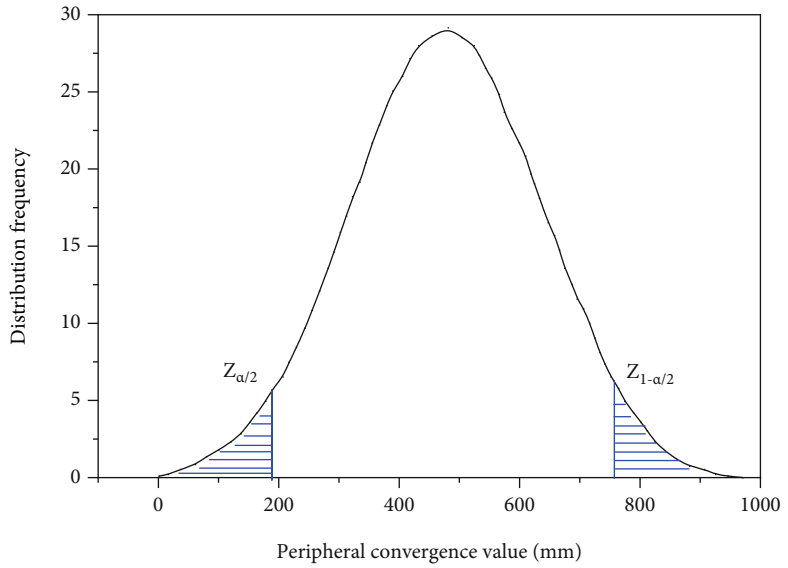

Figure 11: Schematic diagram of tunnel deformation interval estimation.

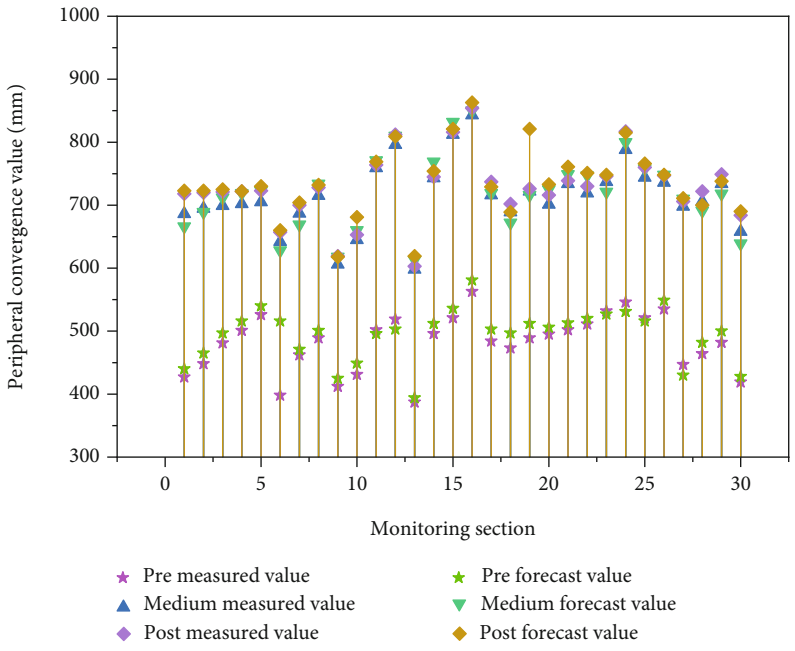

Figure 12: Prediction results of convergence around the tunnel.

Figure 13: Internal force of arch frame and deformation of arch foot.

Table 5: Comparison of design and optimization of original tunnel construction support parameters.

Surrounding rock grade	Geological conditions	Primary support	Reserved deformation	Secondary lining
Original V	Generally buried deep and moderately weathered	C25 shotcrete 26 cm, I20b steel frame spacing 50 cm/frame, 3.0 m long φ 22 hollow anchor rod with longitudinal circumferential spacing of 80 and 100 cm	600 mm	40 cm thick C30-reinforced concrete
Original $V^{strengthen}$	Deep buried strong weathering	Spray C30 concrete for 30 cm and hang HPB 300 φ 8 reinforcement mesh, I22b steel frame, spacing 50 cm/frame, 3.5 m long φ 25 hollow anchor rod with longitudinal circumferential spacing of 50 and 80 cm	800 mm	50 cm thick C30-reinforced concrete
Optimized V	Generally buried deep and moderately weathered	Spray C30 concrete for 30 cm and hang HPB 300 φ 8 reinforcement mesh, I22b steel frame, spacing 50 cm/frame, 3.5 m long φ 25 hollow anchor rod with longitudinal circumferential spacing of 50 and 80 cm	700 mm	50 cm thick C30-reinforced concrete
Optimized $V^{strengthen}$	Deep buried strong weathering	Spray C40 concrete 32 cm, hang HPB300 φ 8 reinforcement mesh, I25b steel frame, spacing 50 cm/frame, 4.0 m long φ 26 hollow anchor rod with longitudinal circumferential spacing of 40 and 80 cm	1000 mm	60 cm thick C35 reinforced concrete

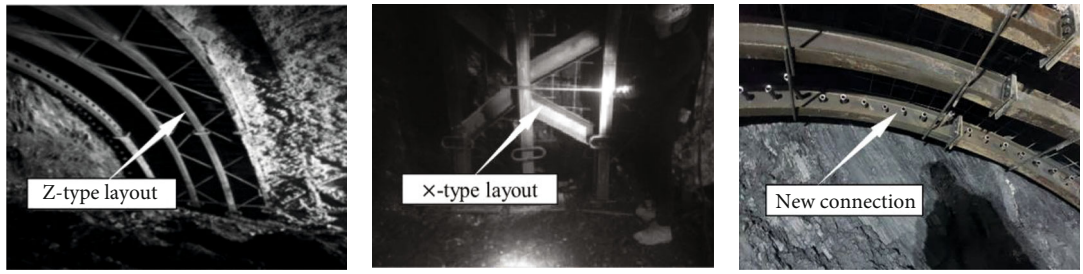

(a) (b) (c)

Figure 14: Optimal design of arch frame.

5.3. Improve the Longitudinal Connection Mode of Arch Frame. The initial support deformation basically starts from the cracking and falling of shotcrete and the desoldering of longitudinal connecting reinforcement, in order to ensure the longitudinal connection strength of I-beam and the integrity of initial support.

(1) The original design is single-layer HRB400 φ 22 connecting bar. In order to improve the integrity of I-beam connection, HRB400 is adopted between steel frames φ 25 reinforcement connected longitudinally, and the circumferential spacing of connecting reinforcement is 1.0 m. The improved arch is arranged according to the double-layer "Z" shape in Figure 14(a)

(2) There is a sudden change when the upper step falls, and the connecting plate is distorted. After the construction of temporary inverted arch, the deformation is restrained, and the deformation of the lower step is small. In order to reduce the sudden change when the step falls, restrain the subsidence deformation during excavation and support at the middle and lower steps, and increase the longitudinal integrity of the steel frame, i18 I-beam shown in Figure 14(b) is used at the 1.0 m position on the arch and wall foot on both sides of the upper and middle steps "×." The I-beam and the steel frame are connected by angle steel or steel plate welding

(3) In tunnel construction, due to the uneven welding level of workers, the previous welding level and welding method cannot meet the construction requirements. By summarizing the longitudinal connection mode, a new connection mode is proposed, as shown in Figure 14(c). Through the use of φ 25 finish rolled deformed steel bars, mechanically connected with nuts, with a circumferential spacing of 1.0 m, when processing the arch, the threaded holes are processed together according to the design spacing. By connecting in this way, human factors are reduced, the perpendicularity and smoothness of arch frames are increased, and the integrity between arch frames is improved

In order to analyze the influence of different steel arch optimization design on the surrounding rock support results in the tunnel, four different support experiments are carried out on four groups of different tunnel sections (d1k87+210, d1k87+215, d1k87+220, and d1k87+225) under the same geological exploration conditions. Among them, d1k87 +210 section adopts traditional steel arch support structure, d1k87+215 section adopts "Z" steel arch support and d1k87 +220 section "X" steel arch support, and d1k87+225 section is supported by traditional steel arch under special welding conditions. The convergence displacement around the tunnel under various steel arch support conditions is shown in Figure 15. From Figure 15, it can be seen that the steel arch has obvious support deformation effect on the surrounding rock in the tunnel after optimized design, the surrounding rock displacement has been significantly improved, and the daily maximum convergence deformation of the surrounding rock has decreased significantly and has decreased from 43.2 mm/d of the traditional steel arch to 35.0 mm/d. Through comparison, it is found that the "X" steel arch support has the best improvement on the overall deformation of surrounding rock, and the final deformation of surrounding rock has also decreased from 783.1 mm to 590.9 mm, a year-on-year decrease of 32.53% compared with the traditional steel arch support. It can be seen that the optimal design of steel arch frame can significantly improve the support effect of surrounding rock, reduce the deformation of surrounding rock, and improve the stability of surrounding rock.

5.4. Reasonably Control the Time, Scope, Location, and Parameters of Initial Support. In the construction of soft and large deformation tunnel, it is necessary to change the old view, and it is appropriate to change the passive reinforcement to active reinforcement. That is, after the initial support construction is completed, pay attention to the anchoring measures behind the tunnel face, and make analysis through monitoring and measurement data, tunnel face sketch, and advanced geological prediction, so as to achieve "measures according to local conditions and tunnel construction strategies," as well as "four reinforcement" considerations: reinforcement time, reinforcement position, reinforcement range, and reinforcement parameters. Through active reinforcement, the deformation is controlled in an effective range.

Active reinforcement time and scope: the traditional tunnel reinforcement time and scope are mostly carried out according to the construction experience. The result is that when the surrounding rock deformation of the tunnel is too large and the deformation time is too long, the

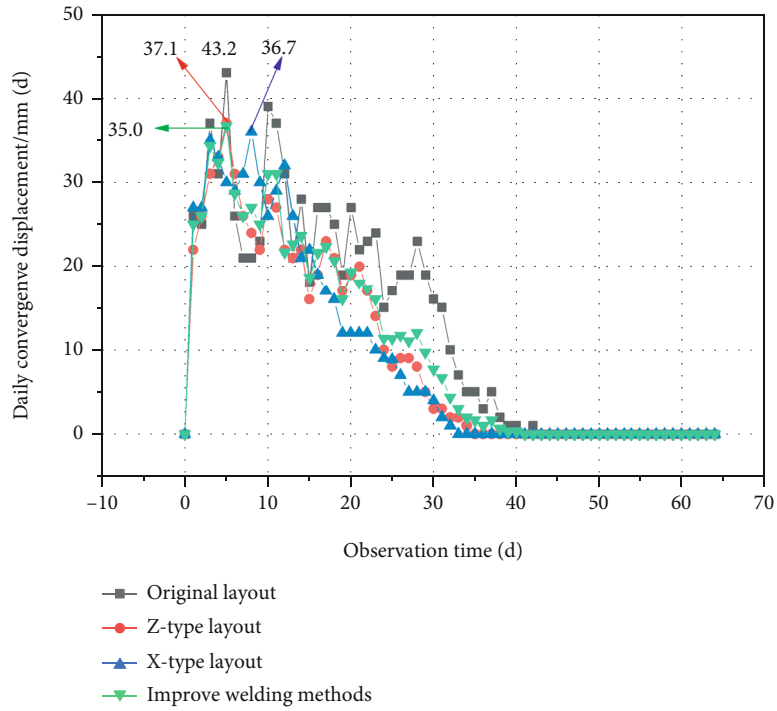

Figure 15: Comparison of convergence values around the tunnel under different arch optimization design.

surrounding rock deformation is not released in time due to the advance support, resulting in all the surrounding rock stress acting on the support structure, resulting in excessive stress and damage to the support structure. Therefore, it can not only provide safe support for the tunnel but also increase the construction cost. On the contrary, when the tunnel surrounding rock deformation is small and the deformation time is short, if it is still carried out according to traditional experience, it may lead to excessive reserved deformation; the support structure cannot play the role of support, resulting in waste of materials and increased construction cost. Therefore, accurate tunnel deformation prediction can not only improve the safety of the tunnel but also reduce the project cost. Therefore, in the construction process of large deformation tunnel, the support structure and support form should be fully selected according to the tunnel deformation prediction results.

6. Conclusions and Suggestions

When a new railway tunnel is built in the carbonaceous slate environment, due to the relatively weak surrounding rock, large deformation is easy to occur in the construction process, which causes great trouble to the construction and operation of the tunnel. Therefore, by expounding the deformation characteristics and characteristics of carbonaceous slate in Wanlamu tunnel and Huajiaopo tunnel, the conclusions are as follows:

(1) In view of the large deformation of tunnel surrounding rock in carbonaceous slate environment, combined with the on-site monitoring means and the intelligent prediction method of tunnel surrounding rock displacement, it has good applicability for the long-term stability analysis and deformation prediction of carbonaceous slate tunnel

(2) Through the analysis of field monitoring data, it is concluded that the deformation characteristics of the railway tunnel are obvious, the deformation time is long, the deformation amount is large, and the maximum value can reach 951.7 mm. There are many influencing factors, including surrounding rock grade, slate bedding, and support mode

(3) The improved GA-BP neural network has strong learning ability in simulating the regression trend of surrounding rock deformation time series. The prediction model optimized by genetic algorithm can effectively avoid the blindness and low efficiency of particle search and improve the prediction accuracy and accuracy of the model for tunnel surrounding rock deformation

(4) On the basis of design, dynamic construction adjustment of tunnel-reserved deformation based on theoretical design and prediction model can effectively avoid the occurrence of surrounding rock collapse or support damage caused by excessive surrounding rock deformation and untimely support or advanced support in the process of tunnel construction

(5) According to the characteristics of surrounding rock, different large deformation lining types are selected for different sections, and the deformation of surrounding rock can be significantly improved, and the convergence deformation of surrounding rock

can be reduced by changing the form of steel arch support structure and increasing the parameters of initial support section steel. Through comparison, it is found that among many optimized steel arch structures, "X" steel arch support has the best improvement on the overall deformation of surrounding rock. The deformation of surrounding rock can be reduced by 192.7 mm, which is 32.53% lower than that of traditional arch support structure

(6) By introducing the concept of timely active support, the passive support parameters are changed into active support parameters, and the passive reinforcement measures are changed into active reinforcement measures, which can effectively slow down the occurrence of surrounding rock displacement, reduce the convergence deformation around the tunnel, and improve the stability of tunnel surrounding rock and support structure

Data Availability

The data used to support the findings of this study are included within the article.

Conflicts of Interest

The authors declare that they have no conflicts of interest.

References

[1] C. Y. Liu Y. Wang et al., "Application of GA-BP neural network optimized by Grey Verhulst model around settlement prediction of foundation pit," *Geofluids*, vol. 2021, Article ID 5595277, 16 pages, 2021.

[2] W. Ren, S. Qiang, X. Wang, Y. Tian, and Z. Li, "Analysis of deformation characteristics of a tunnel in layered soft rocks with considering the effect of bedding," *IOP Conference Series: Earth and Environmental Science*, vol. 570, no. 5, article 052073, 2020.

[3] S. Jun and P. Xiaoming, "Study on nonlinear rheological mechanical characteristics of large deformation of tunnel soft surrounding rock extrusion," *Journal of rock mechanics and engineering*, vol. 31, no. 10, pp. 1957–1968, 2012.

[4] X. Yan and Y. S. Ye, "Research on test of reducing deformation of soft rock tunnel with high stress level by pilot heading," *Applied Mechanics & Materials*, vol. 170-173, pp. 1565–1568, 2012.

[5] S. Weidong, W. Xin, D. Jianhua, and W. Shan, *Research on the Deformation Law of Soft Rock Roadway in High-Stress Area in an Underground Iron Mine*, 2010.

[6] G. Li, Y. Hu, S. M. Tian, M. weibin, and H. L. Huang, "Analysis of deformation control mechanism of prestressed anchor on jointed soft rock in large cross-section tunnel," *Bulletin of Engineering Geology and the Environment*, vol. 80, no. 12, pp. 9089–9103, 2021.

[7] W. Yunlong and T. Zhongsheng, "Structural instability analysis and preventive measures of Muzhailing slate tunnel collapse," *Geotechnical mechanics*, vol. 33, pp. 263–268, 2012.

[8] L. Jun, "Characteristics and cause analysis of large deformation of soft rock in Maoyushan tunnel," *Railway construction*, vol. 8, p. 3, 2013.

[9] X. D. Zhang, P. T. Zhao, and W. J. Gu, "Comparison and analysis of different excavation methods in soft rock-extremely soft rock tunnel," *Applied Mechanics & Materials*, vol. 256, pp. 1201–1205, 2012.

[10] K. Takeda, S. Ohba, and K. Fujita, *Excavation By T.B.M Method In Soft-Rock Tunnels*, 1990.

[11] C. Y. Liu L. Du et al., "A New Rock Brittleness Evaluation Method Based on the Complete Stress-Strain Curve," *Lithosphere*, vol. 2021, no. Special 4, p. 4029886, 2021.

[12] M. Iwano, *Numerical Simulation of Rockmass Behavior around the Shaft Excavated by Short-Step Method*, 2008.

[13] X. L. Guo, Y. Q. Zhu, Z. S. Tan, L. Li, A. Li, and Y. T. Yan, "Research on support method in soft rock tunnel considering the rheological characteristics of rock," *Arabian Journal of Geosciences*, vol. 14, no. 23, pp. 1–14, 2021.

[14] H. Wu, X. Yang, S. Cai, B. Zhao, and K. Zheng, "Analysis of stress and deformation characteristics of deep-buried phyllite tunnel structure under different cross-section forms and initial support parameters," *Advances in Civil Engineering*, vol. 2021, Article ID 8824793, 14 pages, 2021.

[15] Y. Z. Ren, J. Du, and L. H. Zhang, "Deformation characteristics of a shallow tunnel in soft rock," *Modern Tunnelling Technology*, vol. 55, no. 2, pp. 84–90, 2018.

[16] Z. Yuan, *Analysis of the Large Deformation Mechanism of Soft Rock Tunnel in Great Fault Area and Construction Controls*, 2015.

[17] Z. Fang, Z. Zhu, and X. Chen, "Research on construction method and deformation control technology of high ground stress interbedded soft rock tunnel," *Journal of Intelligent and Fuzzy Systems*, vol. 40, no. 6, pp. 1–9, 2020.

[18] F. Pan and S. G. Cheng, "Analysis of deformation mechanism and control technology of soft rock tunnel with high geostress," *Applied Mechanics & Materials*, vol. 638, pp. 794–797, 2014.

[19] C. Li, Y. Zhang, C. Liu, H. Song, and K. Li, "Optimization of tunnel construction parameters in soft rock section with high geostress," *IOP Conference Series: Earth and Environmental Science*, vol. 587, no. 1, article 012074, 2020.

[20] Z. Li and X. Wang, "Study on deformation failure and control strategy for deep large span soft rock roadway," in *International Conference on Information Computing and Applications*, Tangshan, China, 2010.

[21] J. Rao, Y. Tao, P. Xiong et al., "Research on the large deformation prediction model and supporting measures of soft rock tunnel," *Advances in Civil Engineering*, vol. 2020, Article ID 6630546, 13 pages, 2020.

[22] X. Ma, Y. Xue, C. Bai, H. Liu, and Y. Yu, "prediction model for deformation risk grade of the soft rock tunnel based on GRA-Extension," *IOP Conference Series Earth and Environmental Science*, vol. 440, no. 5, article 052057, 2020.

[23] K. Bian, X. Zheng, Y. He, and J. Liu, "Behavior of large deformation and supporting measures in soft rock tunnel," in *Applied Mechanics and Civil Engineering VI*, pp. 9–16, CRC Press, 2017.